Ultrathin g-PAN/PANI encapsulated Cu nanoparticles decorated on $SrTiO_3$ with high stability and as an efficient photocatalytic H_2 evolution and degradation of 4-nitrophenol

Nan Sun,‡ Yong Zhang,‡ Xinru Li, Yuhan Jing, Zhengdong Zhang, Yu Gao, Jianqi Liu, Honglin Tan,* Xiaoming Cai, Jinming Cai

Faculty of Materials Science and Engineering, Kunming University of Science and Technology, Kunming, Yunnan 650000, PR China

‡ These authors contributed equally to this work.

*Corresponding Authors: Dr. Honglin Tan, Faculty of Materials Science and Engineering, Kunming University of Science and Technology, Kunming, Yunnan 650000, PR China.

Email: 852419171@qq.com

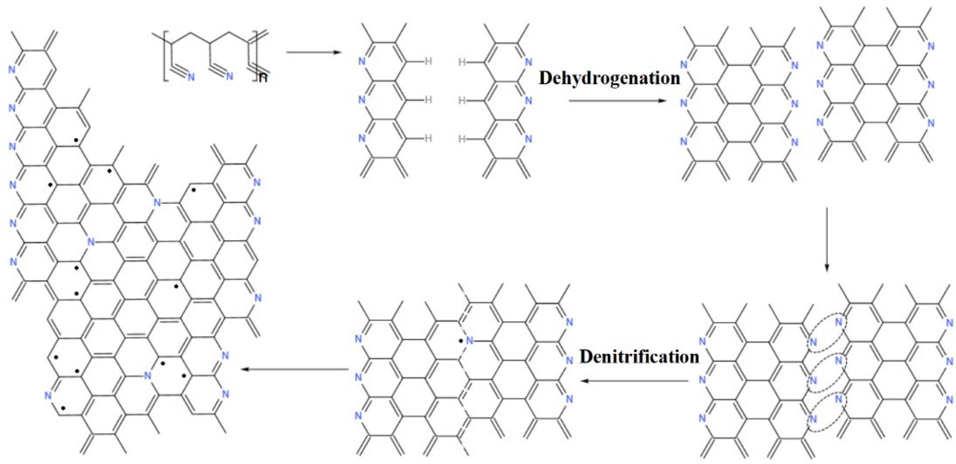

Fig. S1 Structure and synthesis process of g-PAN.

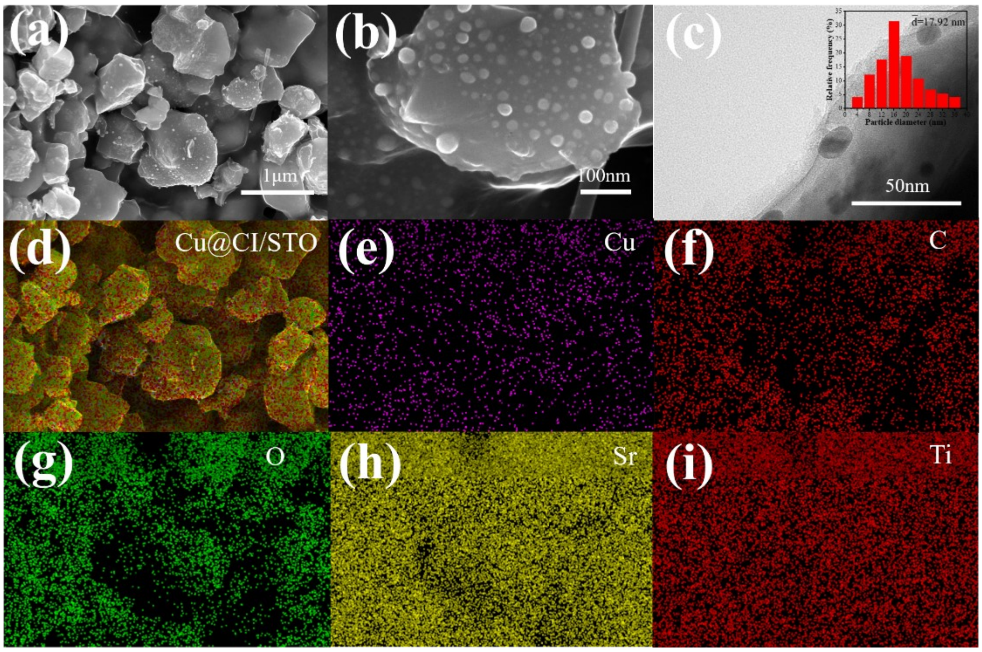

Fig. S2 (a-b) SEM image (c) TEM of Cu@CI/STO-60ml (The illustration shows the Cu NPs particle size); (c-i) corresponding element distribution.

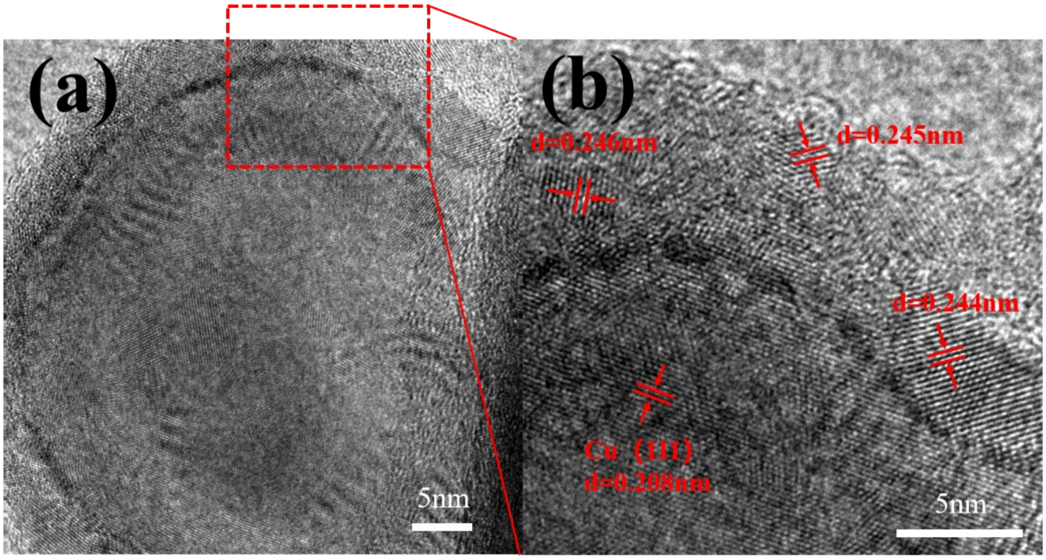

Fig. S3 (a) TEM images of the Cu@CI/STO-10ml structure; (b) HRTEM images of the Cu@CI/STO-10ml structure.

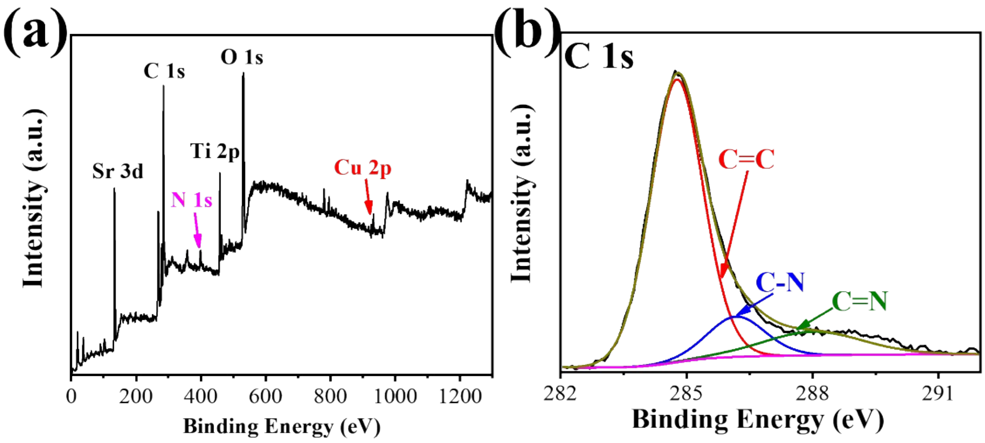

Fig. S4 (a) Complete survey spectrum of the Cu@CI/STO, (b) XPS spectra of C 1s.

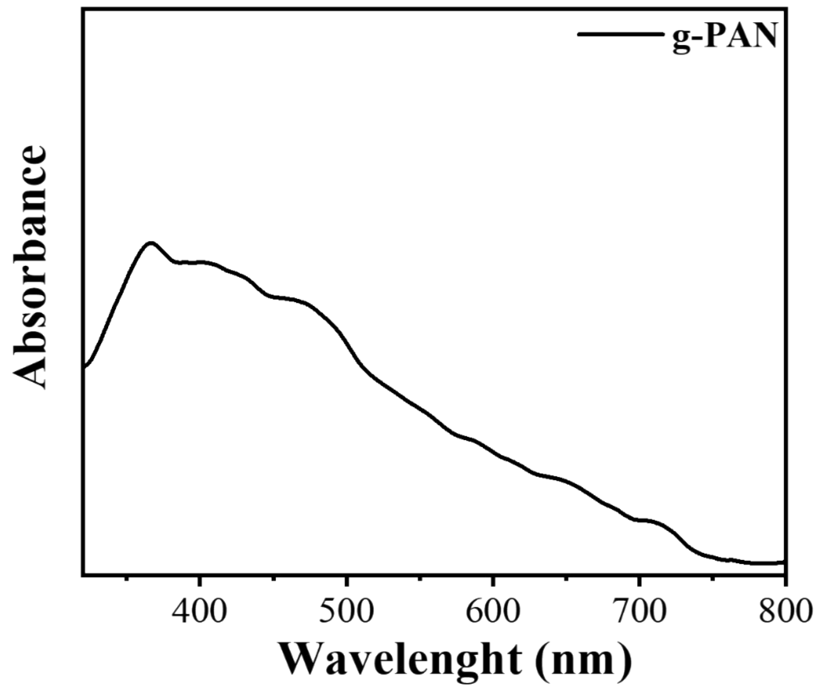

Fig. S5 UV-Vis absorption spectra of g-PAN.

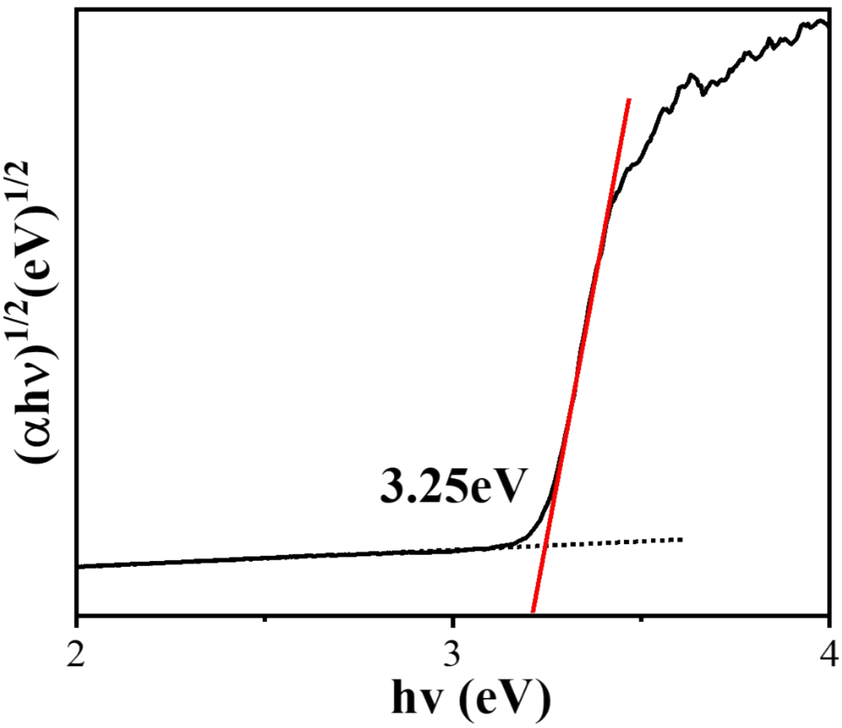

Fig. S6 Tauc plot of $SrTiO_3$.

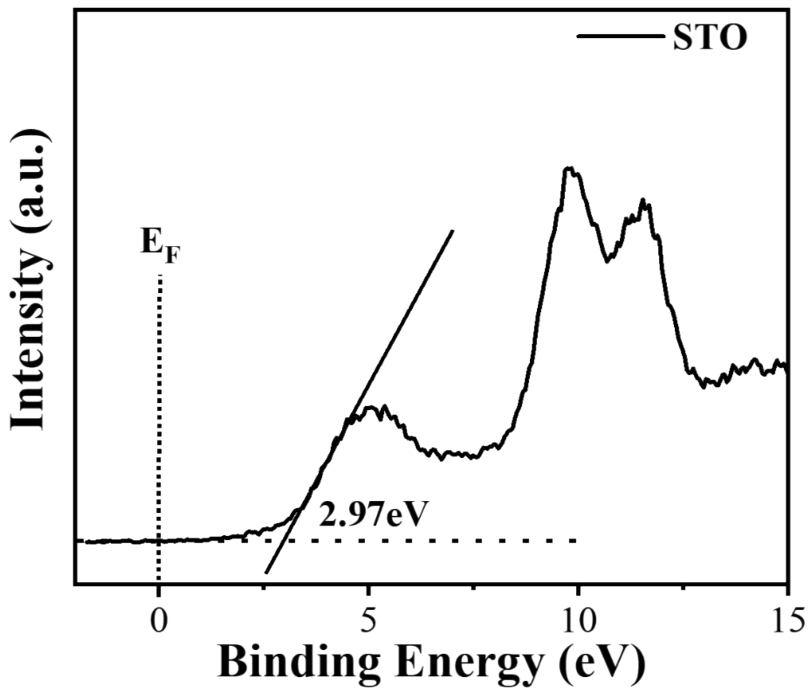

Fig. S7 Tauc plot of Valence band XPS spectrum of $SrTiO_3$.

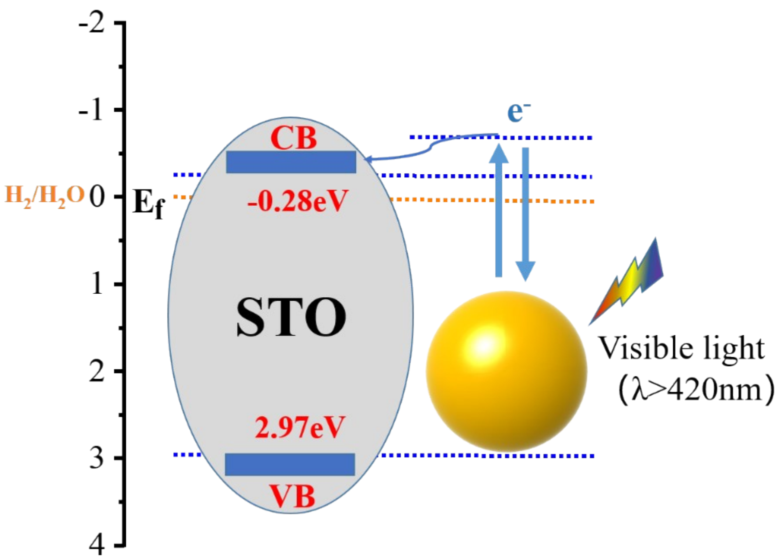

Fig. S8 Schematic illustration of energy band position in $Cu/SrTiO_3$ composite nanostructure.

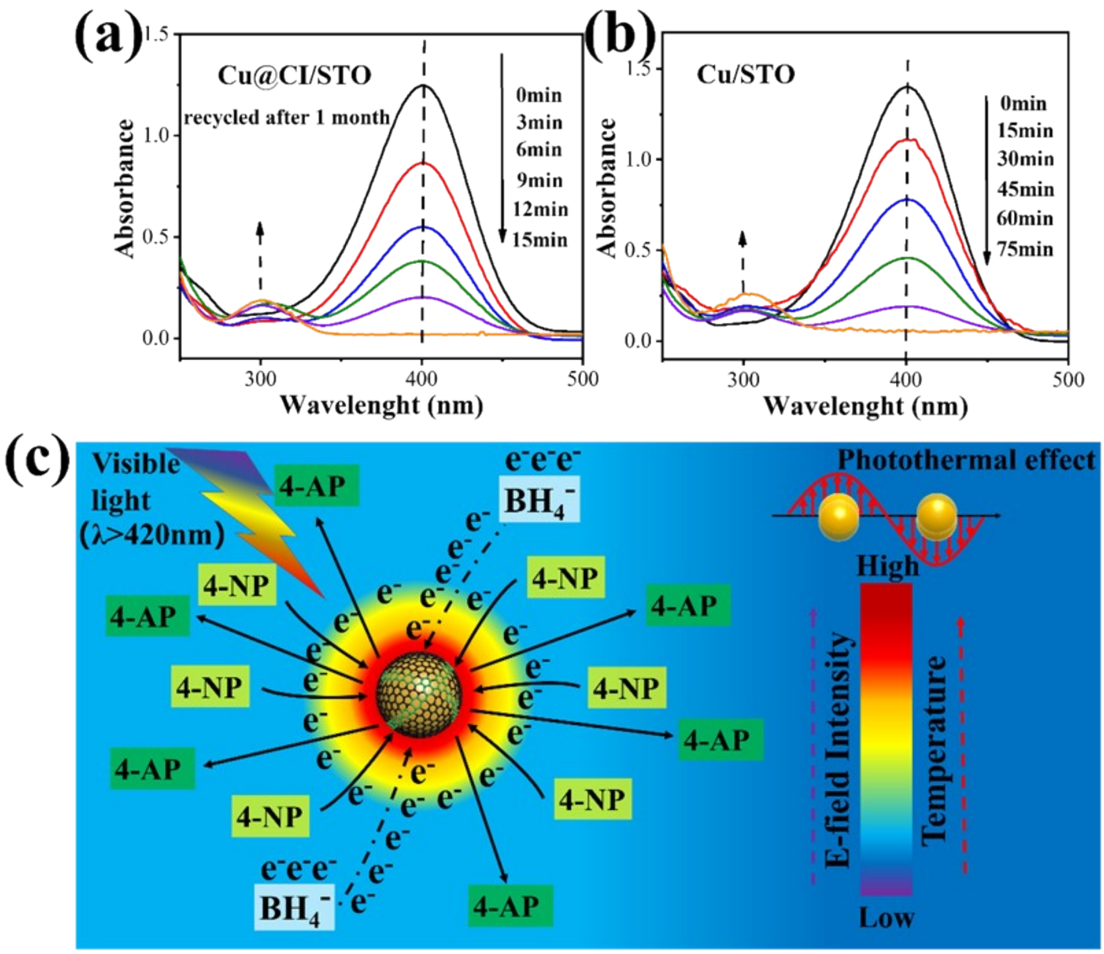

Fig. S9 UV–vis absorbance spectra during the 4-nitrophenol reduction, in presence of (a) Cu@CI/STO, (b) Cu/STO. (c)Schematic diagram of the enhancement of 4-NP catalytic reduction on Cu@CI/STO by the thermal effect of SPR excitation when $NaBH_4$ is used as the electron donor.

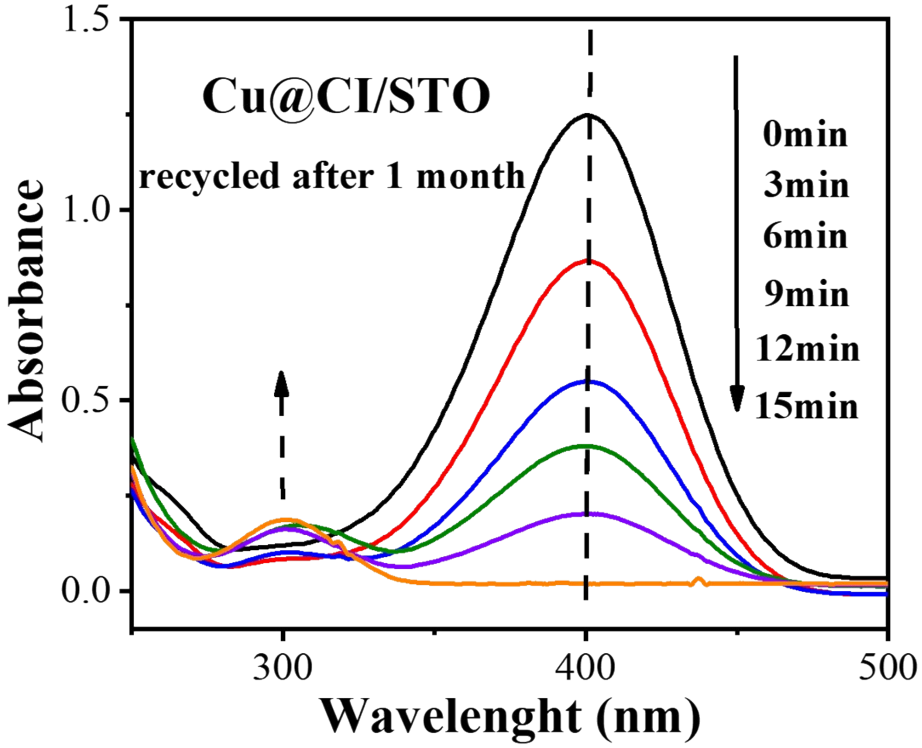

Fig. 10 The UV-Vis absorption spectrum of 4-nitrophenol reduction in the presence of Cu@CI/STO after being placed in the air for 1 month.

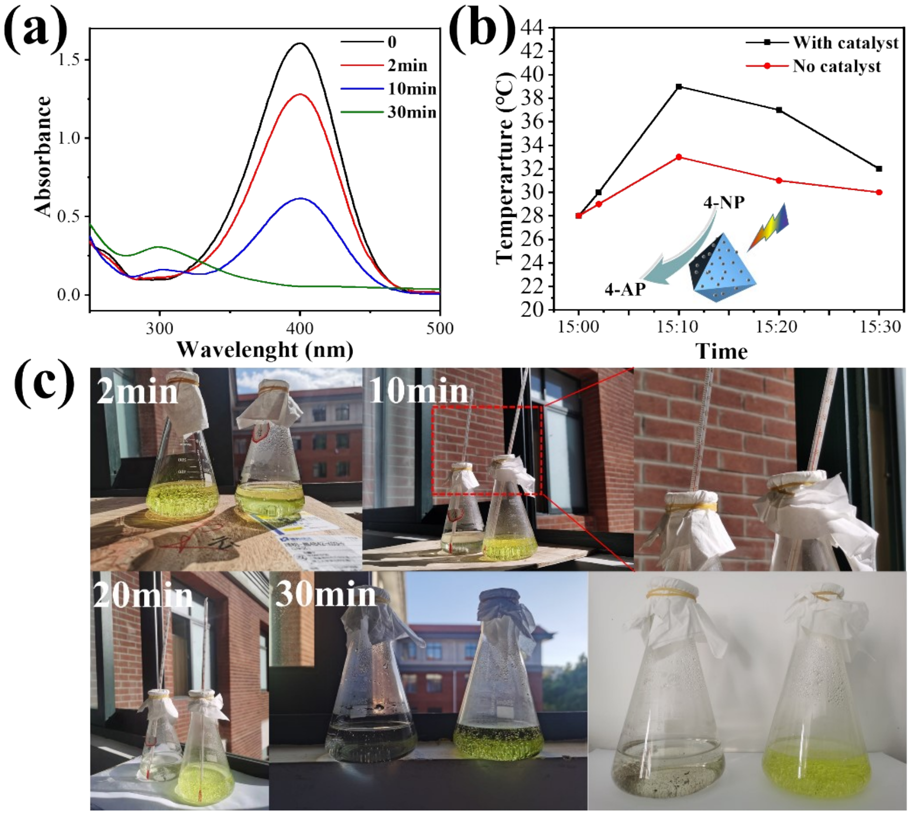

Fig. 11 (a) UV–vis absorbance spectra during the 4-nitrophenol reduction in presence of Cu@CI/STO under sunlight; (b) with or without Cu@CI/STO temperature change with time at different times under sunlight; (c) the image is reflected at different times

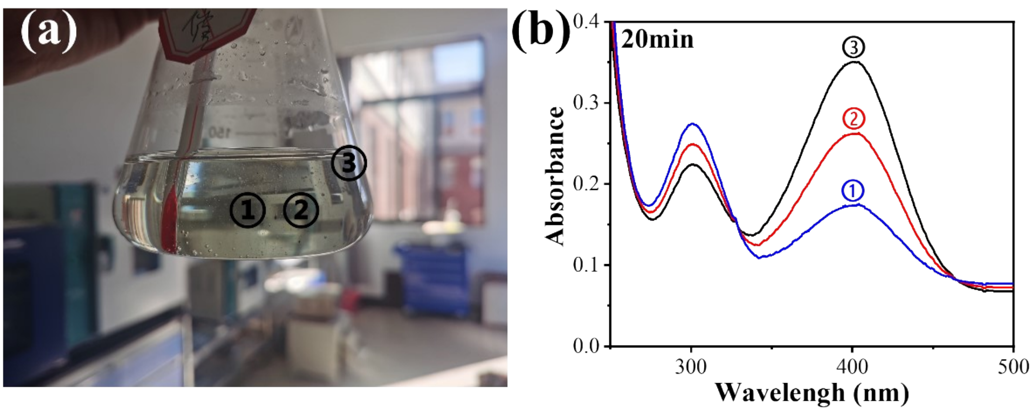

under sunlight.

Fig. 12 Reaction for 20min at (a) different locations and (b) corresponding UV-vis absorbance spectra.

Table. S1 Different materials for metal-driven visible-light photocatalytic hydrogen evolution at present.

Samples	Test condition	Hydrogen production reaction ($\mu mol \cdot g^{-1} \cdot h^{-1}$)	Reference
STO	10% TEOA / 1% Pt /(λ> 420 nm)	5.31	
Au_3Cu/STO	20% methanol/ 0.5% Pt /(λ> 400 nm)	76.3	1
Au nanostar@TiO_2	20% methanol /(λ> 420 nm)	76.6	2
Cu@C/STO	20% methanol/ 0.5% Pt /(λ> 400 nm)	255.3	3
Cu@g-PAN/STO	10% TEOA / 1% Pt /(λ> 420 nm)	265.25	
Cu@CI/STO	10% TEOA / 1% Pt /(λ> 420 nm)	371	This work

References

1 Xz A , Ao F B , Xin C A , et al. Catalysis Today. 2019, **335** 166-172.

2 B. Liu, Y. Jiang, Y. Wang, S. Shang, Y. Ni, N. Zhang, M. Cao, C. Hu, Catal.

Sci. Technol. 2018, **8** 1094-1103.

3 Ren L , Tong L , Yi X , et al. Chemical Engineering Journal. 2020, **390** 124558-.